

Learning Speaker-Invariant Visual Features for Lipreading

Yu Li, Feng Xue, Shujie Li, Jinrui Zhang, Shuang Yang, Dan Guo, Richang Hong

Abstract

Lipreading is a challenging cross-modal task that aims to convert visual lip movements into spoken text. Existing lipreading methods often extract visual features that include speaker-specific lip attributes (e.g., shape, color, texture), which introduce spurious correlations between vision and text. These correlations lead to sub-optimal lipreading accuracy and restrict model generalization. To address this challenge, we introduce SIFLip, a speaker-invariant visual feature learning framework that disentangles speaker-specific attributes using two complementary disentanglement modules (*Implicit Disentanglement* and *Explicit Disentanglement*) to improve generalization. Specifically, since different speakers exhibit semantic consistency between lip movements and phonetic text when pronouncing the same words, our implicit disentanglement module leverages stable text embeddings as supervisory signals to learn common visual representations across speakers, implicitly decoupling speaker-specific features. Additionally, we design a speaker recognition sub-task within the main lipreading pipeline to filter speaker-specific features, then further explicitly disentangle these personalized visual features from the backbone network via gradient reversal. Experimental results demonstrate that SIFLip significantly enhances generalization performance across multiple public datasets. Experimental results demonstrate that SIFLip significantly improves generalization performance across multiple public datasets, outperforming state-of-the-art methods.

CCS Concepts

• Computing methodologies → Computer vision.

Keywords

Lipreading, Feature Disentanglement, Common Feature, Lip motion.

1 Introduction

Lipreading aims to accurately recognize spoken text by analyzing lip movements, regardless of the presence of audio [30]. This field has attracted significant attention due to its potential applications in areas such as silent translation and public safety [40]. In recent years, significant advancements in deep learning have greatly improved lipreading performance [6, 18].

Lipreading methods can be divided into word-level [7, 32] and sentence-level [1, 8, 10, 19, 28] categories. Word-level lipreading focuses on recognizing isolated words, while sentence-level lipreading aims to understand the semantics of continuous lip movement sequences. This study primarily focuses on the latter, which involves more complex modeling due to longer temporal dependencies and richer semantic information. Existing sentence-level lipreading methods typically adopt deep learning frameworks, wherein the front-end adopts deep neural networks to extract visual features, and the back-end decodes these features into text. Various approaches have been proposed to improve model performance. For

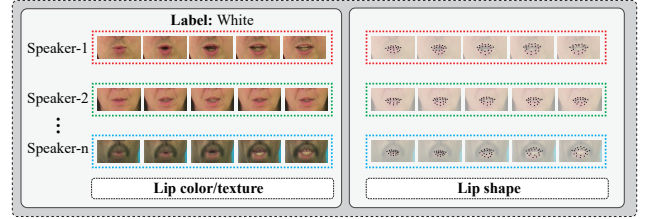


Figure 1: Different speakers exhibit significant visual variations in lip color/shape when pronouncing the same word ‘white’. These speaker-specific visual features limit the generalization of the model.

example, LipNet [4] was the first end-to-end sentence-level lipreading method, enabling continuous sentence prediction and laying the foundation for subsequent research. Zhang *et al* [46] proposed learning audio-visual speech representations by modeling cross-modal shared, unique, and synergistic information. However, these methods often overlook the issue of generalization. As highlighted and empirically validated in [17], the features learned by lipreading models often contain speaker-specific information, which significantly hinders their ability to generalize to *unseen speakers* (speakers who are not present in the training set) [24]. This challenge forms the primary motivation of our work. The root of this problem lies in the considerable variations in lip shape/color across speakers, as shown in Figure 1. Consequently, existing methods tend to extract visual features that inadvertently encode speaker-specific attributes, leading to spurious correlations between visual features and text. This impairs the model to accurately capture common visual features essential for speech content, i.e., speaker-invariant visual features, which in turn impacts its generalization ability. To mitigate speaker variability, Kim [17] proposed a speaker-adaptive lipreading method based on user-dependent padding, which incorporates speaker-specific cues into the padding regions of convolutional layers without modifying the pretrained weights. While this method provides a lightweight adaptation mechanism, it still depends on injecting speaker-specific information. To address this fundamental limitation, our work focuses on decoupling speaker-specific visual features to learn more robust speaker-invariant representations across diverse speakers.

Learning clean and sufficiently informative lip visual features is essential for improving the generalization of lipreading models. In [17], research shows that emphasizing speaker-invariant visual features during encoding and capturing the common features of different speakers when pronouncing the same text can effectively improve generalization. The key to learning speaker-invariant lip visual features lies in effectively filtering out and disentangling speaker-specific features during network training while preserving recognition accuracy. To this end, in this paper, we propose a novel lipreading framework that learns speaker-invariant visual features

by exploring both implicit and explicit disentanglement to decouple speaker-specific features in the backbone network.

In the speaker-specific features *implicit disentanglement* module, we extract speaker-invariant visual feature by aligning spoken text with the visual features of different speakers, thereby improving lipreading accuracy. Since learning speaker-invariant visual features essentially involves filtering out speaker-specific visual (lip color/shape), this can be considered as a form of *implicit disentanglement* of speaker-specific features. Considering the one-to-many mapping between the same spoken text and the visual features of different speakers, inspired by the cross-modal alignment strategy in CLIP [33], we employ cross-modal contrastive learning to align the visual features of different speakers towards a fixed textual vector space, with the goal of learning speaker-invariant features. In lipreading, the subtle temporal variations in a speaker's lip movements (e.g., tongue positioning, lip aperture) evolve continuously across frames. Each frame's visual information carries critical features for distinguishing phonemes or word boundaries, directly impacting semantic understanding. Existing video pre-trained models (e.g., Video CLIP) [9, 13] rely on coarse-grained cross-modal contrastive learning (e.g., global video-text alignment), which works for action classification but fails to achieve the frame-wise alignment essential for lipreading. To address this, we propose a frame-level label cross-modal alignment strategy, which forces the model to establish precise visual-semantic mappings by assigning corresponding text labels to each frame. This fine-grained supervision mechanism compels the model to learn high-quality text-aligned representations, significantly enhancing decoding capabilities for continuous lip movements while improving both recognition accuracy and generalization.

We further design an *explicit disentanglement* module to eliminate potential residual speaker-specific features that may remain after the implicit disentanglement process. The core idea is to first filter out speaker-specific features and then disentangle them from the backbone network. To achieve this, we first design a speaker identification sub-task within the lipreading framework to filter out speaker-specific features. Specifically, the visual features extracted by the visual encoder in the backbone network are used for speaker classification, which guides the model to identify speaker-specific features that are strongly associated with speaker identity (e.g., lip shape). Subsequently, we incorporate a gradient reversal layer to invert the gradient of the speaker identification loss, forcing the visual encoder in the backbone to suppress speaker-specific features when updating its parameters. This explicit disentanglement process further improves the generalization of visual representations across different speakers.

The main contributions of this paper are summarized below:

- 1) We highlight the importance of disentangling speaker-specific features and learning speaker-invariant visual features to improve the generalization of lipreading models.
- 2) We propose a framework SIFlip that learns speaker-invariant visual features for lipreading, which disentangles speaker-specific features by designing both explicit and implicit disentanglement modules, enabling the model to learn common features associated with spoken text, improving the generalization of the lipreading model to unseen speakers.

- 3) We conducted extensive experiments on two benchmark lipreading datasets to validate the effectiveness of the proposed SIFlip model.

2 Related Work

In this section, we first briefly review deep learning-based lipreading methods. We then introduce feature disentanglement techniques and related methods for cross-modal learning.

2.1 Deep Learning-based Lipreading Methods

Lipreading, which converts video to text by analyzing lip movements, has advanced significantly with deep learning frameworks [25, 27, 31, 35]. Existing lipreading methods primarily focus on modifying neural network architectures to improve accuracy. For example, LipNet [4] is the first end-to-end lipreading model capable of continuous sentence recognition. To better capture global semantics across video frames, attention mechanisms have been incorporated into lipreading models [36, 42, 44, 47], improving the ability to track subtle lip movements. Transformer-based architectures [2, 15, 21, 26] further advance lipreading by enabling parallel training and faster convergence compared to RNN, with LipCH-Net [45] being the first Transformer-based Chinese lipreading model.

The existing deep learning-based methods have achieved good recognition performance, but their generalization still has certain limitations, especially when it comes to speakers who have not appeared in the training set, the error rate is relatively high. In this paper, we propose learning speaker-invariant visual features to improve model generalization.

2.2 Feature Disentanglement

Feature disentanglement [29, 39, 41] improves generalization by separating domain-invariant (e.g., speaker-invariant features) and domain-specific (e.g., speaker-specific features) components. For example, in object detection, Liu *et al.* [22] applied feature disentanglement at global and local levels to remove source domain-specific information. Similarly, Deng *et al.* [12] proposed an informative feature disentanglement module to separate high-level semantic features from both source and target domains, improving alignment in unsupervised domain adaptation. In face representation, Bortolato [5] proposed a feature disentanglement autoencoder PFRNet to suppress sensitive attributes, such as gender.

For lipreading, speaker-specific features hinder model generalization. We improve generalization by disentangling speaker-specific visual features to learn speaker-invariant representations.

2.3 Cross-Modal Learning

To enhance cross-modal understanding between visual and textual modalities, recent works [20, 23, 34, 38] have proposed using text as a supervisory signal to improve the representation of visual features. For instance, Radford *et al.* [33] proposed CLIP, which jointly pre-trains an image and text encoder by predicting correct image-text pairs. Similarly, Fang *et al.* [13] introduced CLIP2Video, which aligns video and text in a shared embedding space to facilitate video-language understanding. In sign language recognition, Zhou *et al.* [49] pre-trained a visual-language model with text supervision to bridge the semantic gap between visual and textual representations.

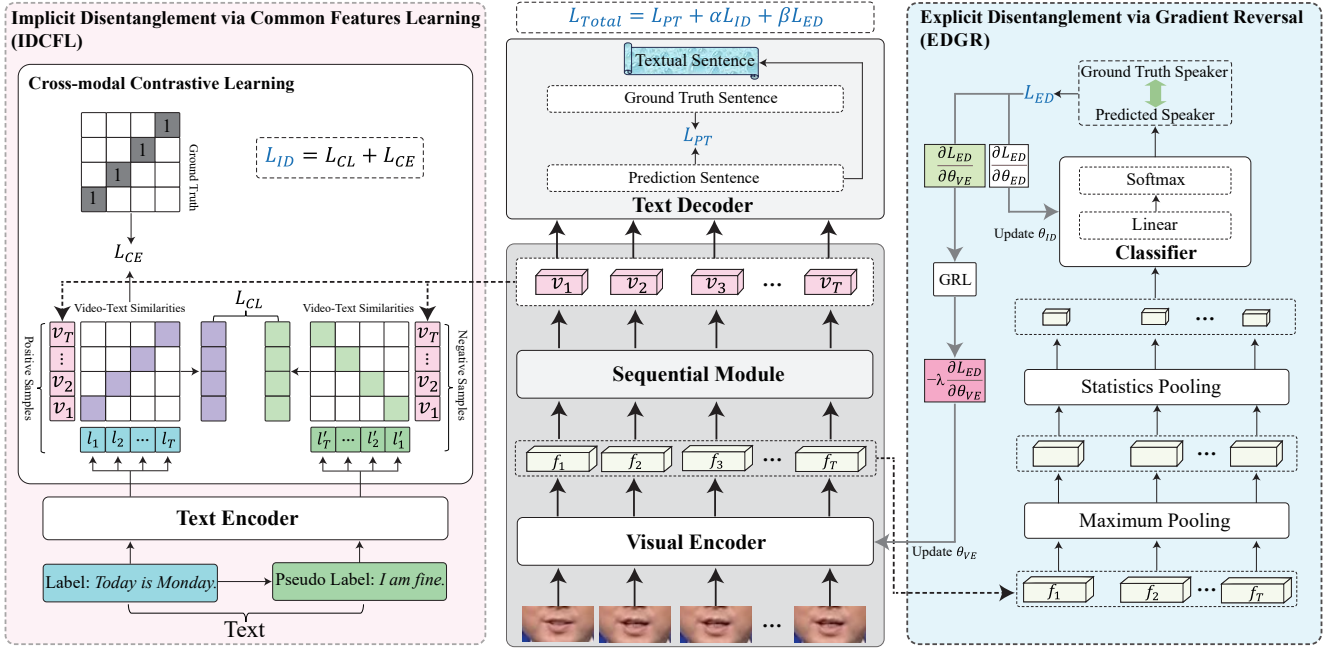


Figure 2: Overview of the proposed SIFlip framework. SIFlip learns speaker-invariant visual features by disentangling speaker-specific features. IDCFL achieves implicit disentanglement by aligning cross-modal features through the calculation of similarity between visual and text features. EDGR achieves explicit disentanglement by reversing the gradient of speaker classification, wherein the classification is based on speaker-specific features filtered through pooling operations. Finally, the visual features are fed into a seq2seq model to be decoded into text.

Lipreading is a cross-modal task that converts video into text. We use text as a stable supervisory signal to learn common features by cross-modal alignment, implicitly disentangling speaker-specific visual features for accurate video-to-text mapping.

3 The Proposed Method

The architecture of the proposed SIFlip is illustrated in Figure 2, which comprising four modules: 1) a visual feature extraction module that extracts visual features of lip region; 2) an implicit disentanglement module (IDCFL) that learns common features aligned with textual semantics to implicitly disentanglement speaker-specific features; 3) an explicit disentanglement module (EDGR) that explicitly filter speaker-specific features and decouples them from the backbone network; 4) a text decoding component that decoding visual features to text.

3.1 Visual Features Extractor

Visual Features Embedding. Given a video clip $X \in \mathbb{R}^{T \times H \times W \times 3}$ with T frames as input, we use 3D-CNN to extract short-term spatiotemporal features of lip movements. After each convolutional layer, ReLU and max pooling are applied. To mitigate overfitting, dropout layers are also included.

Sequential Module. The sequential module captures temporal dependencies in visual features $f = \{f_1, \dots, f_T\}$ extracted by the 3D-CNN. We first use a bidirectional GRU to capture both forward and backward temporal information from the visual features, modeling

the dynamic features of lip movements:

$$f_i = [\vec{f}_i, \overleftarrow{f}_i]. \quad (1)$$

To facilitate information exchange, we further append a 6-layer Transformer after the 3D-CNN and Bi-GRU to model the long-term temporal dependencies of the visual features:

$$v_i = \text{Encoder}(f_i + \text{PE}_{1:T}) \in \mathbb{R}^{T \times d}, \quad (2)$$

where PE denotes Position Encoding, d is the dimensionality of the visual embedding vectors.

3.2 Implicit Disentanglement via Common Features Learning (IDCFL)

Due to the inherent semantic consistency between lip movements and their corresponding text when different speakers pronounce the same words, we design a cross-modal consistency learning module to obtain speaker-independent visual feature representations of lip movements. Specifically, within the multi-modal embedding space, we enforce visual-text alignment and use text-stabilized embeddings as supervisory signals to learn common visual features across speakers, thereby implicitly disentangling and eliminating speaker-specific visual attributes.

To achieve fine-grained semantic alignment between lipreading videos and text, we propose a frame-level label cross-modal alignment method that assigns corresponding text labels to each video frame, establishing a frame-by-frame semantic mapping relationship. Specifically, given a video-text pair $\langle X, t \rangle$, we construct a

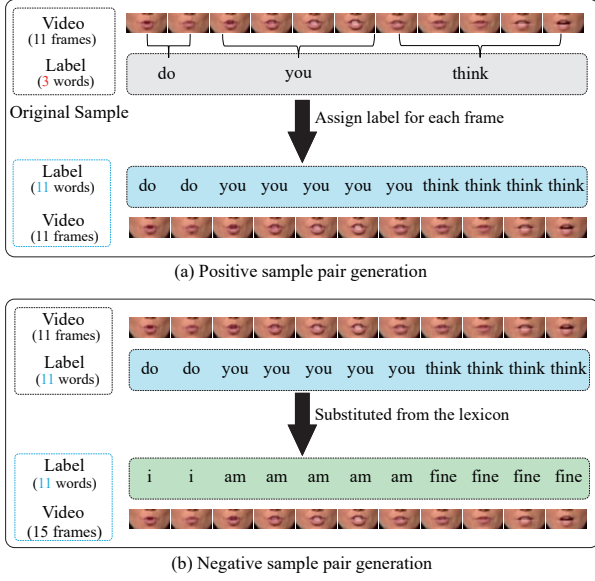


Figure 3: Illustration of positive and negative sample pair generation. Each frame is assigned a corresponding label based on word boundaries in the video frames, forming a positive video-text pair. The negative sample pair is generated by replacing all labels in the positive sample pair.

positive pair $\langle X, L \rangle$ and a negative sample pair $\langle X, L' \rangle$. By learning cross-modal alignment in a multimodal joint embedding space, the model effectively achieves accurate video-text matching. Since text features remain stable regardless of speaker differences, text serves as a reliable supervisory signal to guide the model in learning common visual features that align with the semantics of the text. During this process, the model implicitly disentangles speaker-specific features, facilitating the extraction of common features.

Positive and Negative Sample Pair Generation. Given a video-text pair $\langle X, t \rangle$, where $X = \{x_1, x_2, \dots, x_T\}$ denotes a video clip, and $t = \{t_1, t_2, \dots, t_n\}$ represents the corresponding text sequence of length n ($n < T$), we first use MFA to determine word boundaries within the video. Each frame is then assigned a label based on these boundaries, yielding a label sequence $L = \{l_1, l_2, \dots, l_T\}$ with length T . This process ensures that the video and text sequences are aligned at the frame level, forming a positive sample pair $\langle X, L \rangle$. As shown in Figure 3 (a), the word boundaries segment the video into different regions, and each frame is assigned a corresponding label from the text sequence, enabling fine-grained supervision for model training.

To create a negative sample, we replace all characters in the labels of the positive sample with alternatives randomly selected from the lexicon, generating pseudo-text sequences. The video clip is then paired with these pseudo-text sequences to form the negative sample pair $\langle X, L' \rangle$, as shown in Figure 3 (b). This replacement results in a mismatch between the text sequence and the video, making the negative sample semantically different from the positive sample.

Text Encoding. We use a Transformer Encoder to extract text features. The text sequence $L = \{l_1, l_2, \dots, l_T\}$ is first mapped to a learnable embedding matrix $Q \in \mathbb{R}^{T \times d}$, with sinusoidal positional encodings added. The combined representations are then passed through an N -layer Transformer Encoder to model the temporal dynamics of the sequence:

$$Q = \text{Embedding}(l_i) \in \mathbb{R}^{T \times d}, \quad (3)$$

$$l_i = \text{Encoder}(Q + \text{PE}_{1:T}) \in \mathbb{R}^{T \times d}. \quad (4)$$

Cross-Modal Similarity. Inspired by CLIP, we first calculate the similarity for the positive sample pair $\left\{ \left(v_i, l_i^{\text{pos}} \right) \right\}_{i=1}^T$ and negative sample pair $\left\{ \left(v_i, l_i^{\text{neg}} \right) \right\}_{i=1}^T$. This results in two similarity matrices $\mathbf{E}_{(v,l)}^{\text{pos}} \in \mathbb{R}^{T \times T}$ and $\mathbf{E}_{(v,l)}^{\text{neg}} \in \mathbb{R}^{T \times T}$. Each element in $\mathbf{E}_{(v,l)}$ represents the similarity between the visual feature v_i and the text feature l_i . **Cross-modal Contrastive Learning.** After obtaining the similarity matrices for both the positive and negative sample pair, we perform contrastive learning between $\mathbf{E}_{(v,l)}^{\text{pos}}$ and $\mathbf{E}_{(v,l)}^{\text{neg}}$, using the InfoNCE loss function to bring together the embeddings of matching image-text pair while separating the embeddings of mismatched image-text pair. This can be formalized as:

$$\mathcal{L}_{CL} = -\frac{1}{T} \sum_{i=1}^T \log \frac{\exp \left(e_i^{\text{pos}} / \tau \right)}{\exp \left(e_i^{\text{pos}} / \tau \right) + \sum_{j=1}^T \exp \left(e_j^{\text{neg}} / \tau \right)},$$

where e_i^{pos} and e_i^{neg} are the diagonal elements of $\mathbf{E}_{(v,l)}^{\text{pos}}$ and $\mathbf{E}_{(v,l)}^{\text{neg}}$, respectively, while τ is a trainable temperature parameter.

To further improve the alignment between visual features and text, we use the cross-entropy loss function to compute the loss between the similarity matrix of the positive sample pair $\mathbf{E}_{(v,l)}^{\text{pos}}$ and the ground truth matrix $\mathbf{E}_{(v,l)}^G$:

$$\mathcal{L}_{CE} = - \sum \mathbf{E}_{(v,l)}^G \log(\mathbf{E}_{(v,l)}^{\text{pos}}) \quad (5)$$

where $\mathbf{E}_{(v,l)}^G$ is a $T \times T$ identity matrix, with ones on the diagonal and zeros in the off-diagonal elements.

We define the above two losses as \mathcal{L}_{ID} , as follows:

$$\mathcal{L}_{ID} = \mathcal{L}_{CL} + \mathcal{L}_{CE}. \quad (6)$$

3.3 Explicit Disentanglement via Gradient Reversal (EDGR)

In addition to the implicit disentanglement module described in Section 3.2, to further disentangle speaker-specific features from the backbone network, we designed an explicit disentanglement module for speaker-specific visual lip features. Specifically, we designed a speaker recognition sub-task within the main lipreading pipeline to filter out speaker-specific visual features. Then, we further explicitly disentangled these personalized visual features from the backbone network via gradient reversal, thereby improving the generalization ability of visual representations across speakers.

To extract speaker-specific visual features, the intermediate feature representation f_i undergoes a series of pooling operations. Initially, max pooling is applied to compress the spatial dimensions,

highlighting salient speaker-specific features and generating the intermediate feature f'_i . Subsequently, statistical pooling is performed by concatenating the mean and standard deviation of f'_i across the temporal dimension, forming a global speaker representation f''_i . This representation is then input into a classifier that computes the prediction probability y' for each speaker. The module is trained with loss \mathcal{L}_{ED} , which is a cross-entropy loss:

$$y' = \text{Softmax}(\text{Linear}(\text{ReLU}(\text{Linear}(f''_i)))) \quad (7)$$

$$\mathcal{L}_{ED} = -\sum_{i=1}^N y_i \log(y'_i), \quad (8)$$

where $y' \in \mathbb{R}^N$, N is the total number of speakers, and y_i denotes the ground truth speaker ID.

To mitigate the influence of speaker-specific features during training, we incorporate a Gradient Reversal Layer (GRL) [14] into the framework based on feature disentanglement principles. Positioned between the feature extractor and speaker classifier, the GRL reverses the gradient of the speaker classification loss, guiding the model to explicit disentanglement speaker-specific features. Formally, let \mathcal{L}_{ED} denote the speaker classification loss. The visual encoder network parameters are denoted as θ_{VE} , and the speaker classifier parameters as θ_{ED} . The overall training is expressed as:

$$\theta_{ED} \leftarrow \theta_{ED} - \eta \frac{\partial \mathcal{L}_{ED}}{\partial \theta_{ED}}, \quad (9)$$

$$\theta_{VE} \leftarrow \theta_{VE} - (-\lambda) \eta \frac{\partial \mathcal{L}_{ED}}{\partial \theta_{VE}}, \quad (10)$$

where η is the learning rate, λ is the parameter.

As the speaker classifier accurately predicts the speaker's ID, the gradient reversal layer forces the model to penalize speaker-specific features, driving the backbone network to explicitly disentangle them.

3.4 Text Decoding via Seq2Seq Model

We adopt a sequence-to-sequence (seq2seq) model [37] to decode visual features into text. The encoder processes the input feature sequence $v = \{v_1, \dots, v_T\}$, generating hidden states h_e^v , while the last hidden state initializes the decoder's GRU. At each time step j , the decoder updates its hidden state h_d^t based on the previous prediction w'_{j-1} and the prior hidden state:

$$(h_e^v)_j = \text{GRU}_e^v((h_e^v)_{j-1}, e^v), \quad (11)$$

$$(h_d^t)_j = \text{GRU}_d^t((h_d^t)_{j-1}, e_{j-1}^t). \quad (12)$$

The encoder output is attended at each time step to compute the context vector $(c_t^v)_j$, which is used to generate the output w . The model is trained with predicted text loss \mathcal{L}_{PT} :

$$(c_t^v)_j = h_e^v \cdot \text{att}((h_d^t)_j, h_e^v), \quad (13)$$

$$P(w) = \text{Softmax}(\text{MLP}((h_d^t)_j, (c_t^v)_j)), \quad (14)$$

where v and t denote the visual and text modalities, respectively.

$$\mathcal{L}_{PT} = -\frac{1}{n} \sum_{i=1}^n \sum_{j=1}^m w_{ij} \log w'_{ij}, \quad (15)$$

where w denote the ground-truth, n is the sequence length, and m is the number of word categories.

In addition, our model can be applied to Chinese datasets. For Chinese dataset, we implement a cascaded seq2seq [43, 47] model

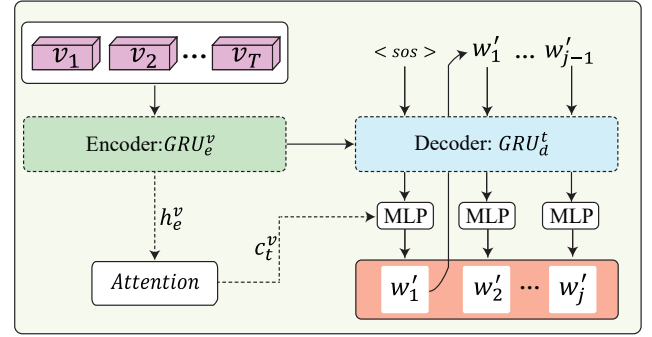


Figure 4: Illustration of Seq2Seq module. The Seq2Seq module with an encoder-decoder structure that decodes visual features into text.

that first predicts pinyin, which is then converted into Chinese characters. Given the limited phonetic forms in pinyin, this intermediate step enhances cross-modal decoding accuracy.

3.5 Model Optimization

To optimize SIFlip, we jointly minimize three loss functions: \mathcal{L}_{PT} , \mathcal{L}_{ED} , and \mathcal{L}_{ID} . The predicted text loss \mathcal{L}_{PT} ensures that the text sequence predicted by the backbone network closely aligns with the ground truth. \mathcal{L}_{ED} facilitates the semantic alignment of visual features extracted by the backbone with text features, implicitly disentangling speaker-specific features. Meanwhile, \mathcal{L}_{ID} guides the branch to filter speaker-specific features, further assisting the backbone in explicitly disentangling them. The total loss is formulated as a weighted sum of these three losses:

$$\mathcal{L}_{Total} = \mathcal{L}_{PT} + \alpha \mathcal{L}_{ID} + \beta \mathcal{L}_{ED}, \quad (16)$$

where α and β are hyperparameters.

4 Experiments

4.1 Experimental Settings

4.1.1 Dataset. We validate the proposed method on two benchmark datasets: CMLR [47] and GRID [11].

CMLR [47] is the largest publicly available Chinese lipreading dataset, includes 11 speakers and over 100,000 sentences. For both unseen and seen speakers, we follow the division method in [43].

GRID [11] is a widely used English lipreading dataset, consisting of 32,823 sentences spoken by 33 speakers. We use the same dataset division method for unseen and seen speakers as in [4].

For the sentence-level datasets CMLR and GRID, Word Error Rate (WER) (%) is used as the evaluation metric [16, 16, 48].

4.1.2 Baselines. To evaluate the effectiveness of our proposed SIFlip, we compared our method with several baselines: LipNet [4], WAS [36], CSSMCM [47], LIBS [48], CALLip [16], LCSNet [44], Ai et.al [2], LipFormer [43].

4.1.3 Implementation Details. For each video clip, we use the DLib face detector [3] to locate facial regions in each frame and extract a 160×80 -pixel mouth-centered crop as input. The visual

Table 1: Performance comparison with state-of-the-art methods on CMLR and GRID. -: results not available. Best results are in boldface. Imp indicates the absolute improvement of SIFLip relative to the best-performing baseline.

Methods	CMLR		GRID	
	Seen Speakers (CER ↓)	Unseen Speakers (CER ↓)	Seen Speakers (CER ↓)	Unseen Speakers (CER ↓)
LipNet[4]	33.41	52.18	4.8	17.5
WAS [36]	38.93	-	3.0	14.6
CSSMCM [47]	32.48	50.08	-	-
LIBS [48]	31.27	-	-	-
CALLip[16]	31.18	-	2.48	-
LCSNet [44]	30.03	46.98	2.3	11.6
Ai <i>et.al</i> [2]	-	-	1.1	-
LipFormer [43]	27.79	43.18	1.45	9.64
SIFLip	20.55	32.16	0.79	6.23
<i>Imp (absolute)</i>	<i>+7.24</i>	<i>+11.02</i>	<i>+0.31</i>	<i>+3.41</i>

encoder comprises a 3-layer 3D-CNN, while the Transformer encoder consists of 6-layer, each with a hidden size of 512 and 8 attention heads. In Eq. (16), we set $\alpha = 0.5$, $\beta = 2.0$ for CMLR and GRID datasets.

The word boundaries in Sec 3.2 are obtained using the MFA (Montreal Forced Aligner). Specifically, MFA aligns audio with text labels to determine the start and end boundaries of each word in the audio. Given audio-video synchronization, this alignment enables accurate localization of the word boundaries in the video. Notably, during training, both video and text were used as inputs, whereas during testing, only video was used.

4.2 Overall Comparison

In this subsection, we compare SIFLip with other typical baselines. LipNet is the basic pipeline for lipreading. However, its CTC loss failed to converge during training on CMLR. Therefore, we replaced CTC with Seq2Seq module. Beyond evaluating seen speakers, we also assessed the model on unseen speakers to measure its generalization.

Results on CMLR dataset. Table 1 compares the proposed SIFLip with baselines. The results show that SIFLip significant performance improvements, particularly for unseen speakers, demonstrating its superior generalization. Specifically, compared to LipFormer, SIFLip achieves absolute improvements of +7.24 for seen speakers and +11.02 for unseen speakers. Moreover, its advantages over other baselines are even more evident. This can be attributed to its ability to disentangle speaker-specific visual features, effectively minimizing the impact of speaker variations.

Results on GRID dataset. As shown in Table 1, SIFLip outperforms all baseline methods, both for seen and unseen speakers. Specifically, LipNet is the earliest lipreading method, achieves a CER of 4.8% for seen speakers, while SIFLip reduces it to 0.79%. WAS and CALLip uses audio-visual bimodal input, SIFLip achieves better performance with visual unimodal input. These improvements are due to SIFLip to learn speaker-invariant visual features.

4.3 Ablation Study

In the overall comparison experiment in Section 4.2, four datasets were used. Since the CMLR dataset is the most representative (it contains speaker identity information, and the spoken texts exhibit

a certain degree of diversity in terms of length and content). Therefore, in this section, we use the CMLR as the test dataset for the ablation study.

4.3.1 Effect of IDCFL and EDGR. We first conduct ablation studies to validate the effectiveness of the IDCFL and EDGR modules in SIFLip. The following three variants are designed:

- *Base*: It is the backbone of SIFLip, consisting of 3D-CNN, GRU, Transformer, and Seq2Seq.
- *Base w/ IDCFL*: It adds the IDCFL module to the Base.
- *Base w/ EDGR*: It adds the EDGR module to the Base.

Table 2: Ablation study of IDCFL and EDGR.

Methods	CMLR	
	Seen (CER ↓)	Unseen (CER ↓)
Base	28.52	47.86
Base w/ IDCFL	21.49	33.13
Base w/ EDGR	26.22	39.02
SIFLip	20.55	32.16

Table 2 summarizes the ablation experiments evaluating the contributions of the IDCFL and EDGR modules in SIFLip, leading to the following observations.

Among all variants of SIFLip, the Base performs the worst, as visual variations result in the extracted features containing substantial speaker-specific features, which limits generalization. In contrast, the performance of Base w/ IDCFL improves significantly. This is attributed to the fact that IDCFL employs text as a supervisor signal, which strengthens the visual-text alignment and guide the model to learn common visual features that are semantically consistent with the text, achieving implicit disentanglement of speaker-specific features. Meanwhile, Base w/ EDGR also outperforms the Base, confirming the effectiveness of the EDGR module in explicitly disentangling speaker-specific features to improving generalization. Notably, Base w/IDCFL achieves better performance than Base w/EDGR, suggesting that learning speaker-independent features aligned with semantic content plays a more critical role in improving generalization for the lipreading task. Finally, SIFLip,

which integrates both IDCFL and EDGR, achieves the best overall performance, highlighting the complementary effects of implicit and explicit disentanglement.

4.3.2 Effect of Joint Loss. We then conducted ablation studies to evaluate the contribution of each disentanglement within the IDCFL and EDGR modules. To achieve implicit disentanglement of speaker-specific features, the IDCFL module performs cross-modal alignment between visual and textual features by incorporating contrastive loss \mathcal{L}_{CL} and cross-entropy loss \mathcal{L}_{CE} . To explicitly disentangle speaker-specific features, EDGR employs a Gradient Reversal Layer (GR), which reverses the gradient of the speaker classification loss \mathcal{L}_{ED} during backpropagation. To assess the impact of each component, we design the following five variants:

- *w/o \mathcal{L}_{CE}* : This variant removes \mathcal{L}_{CE} in Eq. (6).
- *w/o \mathcal{L}_{CL}* : This variant removes \mathcal{L}_{CL} in Eq. (6).
- *w/o \mathcal{L}_{ID}* : This variant removes \mathcal{L}_{ID} in Eq. (16), which is equivalent to removing the entire IDCFL module.
- *w/o GR*: This variant removes GR from EDGR.
- *w/o \mathcal{L}_{ED}* : This variant removes \mathcal{L}_{ED} from EDGR, which renders the GR layer ineffective and disables the entire EDGR module.

The detailed results of these ablation studies are shown in Table 3, leading to the following observations.

For the IDCFL module, *w/o \mathcal{L}_{CL}* results in lower performance than SIFlip, indicating that the contrastive learning in SIFlip improve the semantic consistency between paired visual and textual features by pulling positive pairs closer and pushing negative pairs apart, significantly improving the discrimination of visual features. The performance of *w/o \mathcal{L}_{CE}* is even lower than that of *w/o \mathcal{L}_{CL}* , indicating that the cross-entropy loss contributes to finer-grained visual-text alignment. *w/o \mathcal{L}_{ID}* leads to substantial performance degradation on both seen and unseen speakers, highlighting the importance of learning visual features that are semantically aligned with text for enhancing overall performance and generalization.

Table 3: Ablation study of joint loss function.

Methods	CMLR	
	Seen (CER ↓)	Unseen (CER ↓)
SIFlip	20.55	32.16
<i>w/o \mathcal{L}_{CL}</i>	22.89	32.95
<i>w/o \mathcal{L}_{CE}</i>	22.95	33.57
<i>w/o \mathcal{L}_{ID}</i>	26.22	39.02
<i>w/o GR</i>	20.96	33.07
<i>w/o \mathcal{L}_{ED}</i>	21.49	33.13

For the EDGR module, *textitw/o GR* exhibits a significant increase in CER for unseen speakers. This suggests that gradient inversion is effective in suppressing speaker-specific features in the backbone network by reversing the speaker classification loss in the case that the classifier is accurate. *w/o \mathcal{L}_{ED}* , which leads to further performance degradation, confirming that the speaker sub-task can effectively filter out speaker-specific features.

4.4 Visualization for IDCFL.

We delve deeper into visualizing the cross-modal alignment attained by the IDCFL module. Specifically, we pick one sample from the CMLR dataset to vividly illustrate the extent of alignment between visual and text features, as presented in Figure 5. In the heatmap, darker hues signify higher similarity and more optimal alignment, whereas lighter hues mirror lower similarity. These outcomes clearly demonstrate the efficacy of IDCFL in accomplishing cross-modal feature alignment.

4.5 Hyperparameter Study

In this subsection, we perform hyperparameter studies on CMLR dataset to evaluate the influence of α and β in Eq. (16) on model performance.

Effect of the Hyper-parameter α . The weight for the Loss \mathcal{L}_{ID} is an important hyper-parameter, as it directly guides the backbone network to learn visual features aligned with the semantics of the spoken text. As shown in Figure 7, the model achieves optimal performance at $\alpha = 0.5$.

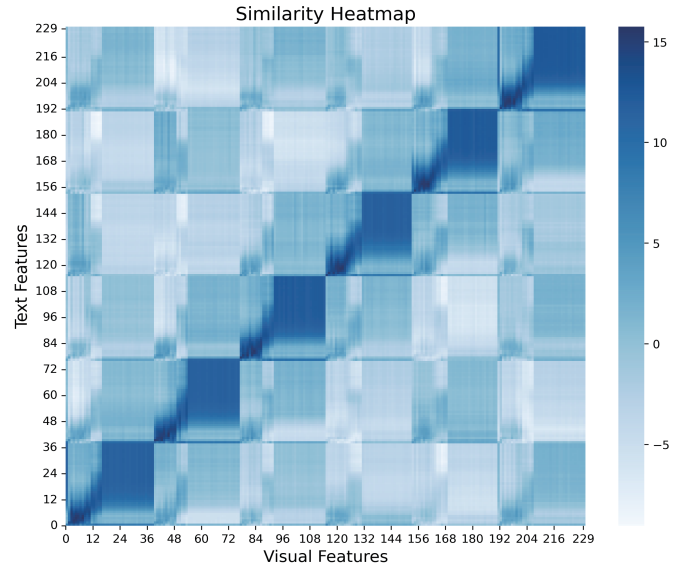


Figure 5: Heatmap of Visual and Text Feature Similarity. The horizontal axis represents visual features and the vertical axis represents text features.

Effect of the Hyper-parameters β . As shown in Figure 7, the model achieves optimal generalization at $\beta = 2.0$. A moderate β effectively suppresses speaker-specific features. However, an overly large value may dominate optimization, hindering the extraction of speech-relevant visual features and degrading performance.

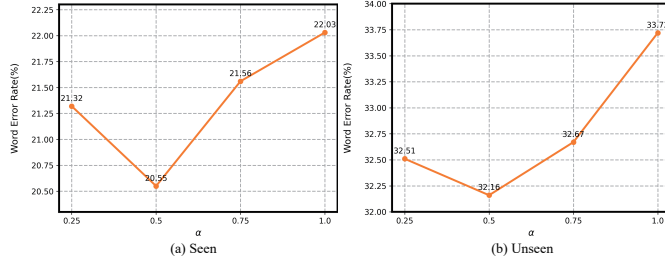


Figure 6: Effects of different hyper parameter α in Eq. (16) on CMLR dataset. (a) Seen speakers. (b) Unseen speakers.

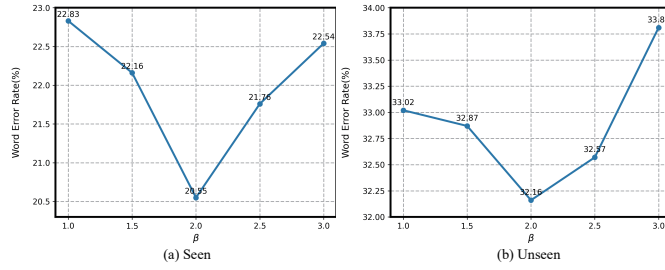


Figure 7: Effects of different hyper parameter β in Eq. (16) on CMLR dataset. (a) Seen speakers. (b) Unseen speakers.

4.6 Case Study

To qualitatively analyze the effectiveness of the proposed model, we visualized one case from CMLR dataset, as shown in Figure 8. The results clearly indicate that the base predictions contain notable errors compared to the ground truth. With incorporates the IDCFL module, prediction accuracy improves significantly. Furthermore, incorporating the EDGR module further improves generalization to unseen speakers.

Label: 我向你们致以热烈的祝贺 (I extend my warm congratulations to you.)

Ground Truth	我	向	你	们	表	示	热	烈	祝	贺
Base	我	相	十	们	表	示	热	烈	祝	贺
Base+IDCFL	我	向	你	们	表	示	热	烈	祝	贺
Base+EDGR	我	向	你	们	表	示	热	烈	祝	贺
SIFLip	我	向	你	们	表	示	热	烈	祝	贺

Figure 8: Visualization of prediction examples on CMLR. Each colored block corresponds to its generated word. Gray blocks indicate prediction errors, and red font highlights word prediction errors.

5 Conclusion

In this paper, we propose SIFLip, a novel lipreading framework designed to enhance model generalization by learning speaker-invariant visual features through dual-branch feature disentanglement. Our method disentangles speaker-specific features via two complementary mechanisms: (1) Implicit disentanglement, which aligns visual features with their corresponding text features to capture speaker-invariant features; and (2) Explicit disentanglement, which employs gradient reversal layers to adversarially suppress

speaker-specific information during feature learning. Comprehensive evaluations on benchmark datasets demonstrate that SIFLip achieves state-of-the-art performance while significantly improving generalization to unseen speakers. In future work, we aim to extend our approach to side-view lipreading scenarios to further enhance its robustness and applicability in real-world situations.

References

- [1] Ahsan Adeel, Mandar Gogate, Amir Hussain, and William M Whitmer. 2019. Lip-reading driven deep learning approach for speech enhancement. *IEEE Transactions on Emerging Topics in Computational Intelligence* 5, 3 (2019), 481–490.
- [2] Xi Ai and Bin Fang. 2023. Cross-Modal Language Modeling in Multi-Motion-Informed Context for Lip Reading. *IEEE/ACM Transactions on Audio, Speech, and Language Processing* 31 (2023), 2220–2232.
- [3] Alessandro Amodio, Michele Ermidoro, Davide Maggi, Simone Formentin, and Sergio Matteo Savaresi. 2018. Automatic detection of driver impairment based on pupillary light reflex. *IEEE transactions on intelligent transportation systems* 20, 8 (2018), 3038–3048.
- [4] Yannis M Assael, Brendan Shillingford, Shimon Whiteson, and Nando De Freitas. 2016. Lipnet: End-to-end sentence-level lipreading. *arXiv preprint arXiv:1611.01599* (2016).
- [5] Blaž Bortolato, Marija Ivanovska, Peter Rot, Janez Krizaj, Philipp Terhörst, Naser Damer, Peter Peer, and Vitomir Struc. 2020. Learning privacy-enhancing face representations through feature disentanglement. In *2020 15th IEEE International Conference on Automatic Face and Gesture Recognition (FG 2020)*. IEEE, 495–502.
- [6] Hugo Bulzomi, Marcel Schweiker, Amélie Gruel, and Jean Martinet. 2023. End-to-end neuromorphic lip-reading. In *Proceedings of the IEEE/CVF Conference on Computer Vision and Pattern Recognition*. 4101–4108.
- [7] Hang Chen, Qing Wang, Jun Du, Gen-Shun Wan, Shi-Fu Xiong, Bao-Ci Yin, Jia Pan, and Chin-Hui Lee. 2024. Collaborative Viseme Subword and End-to-End Modeling for Word-Level Lip Reading. *IEEE Transactions on Multimedia* 26 (2024), 9358–9371.
- [8] Xuejuan Chen, Jixiang Du, and Hongbo Zhang. 2020. Lipreading with DenseNet and resBi-LSTM. *Signal, Image and Video Processing* 14 (2020), 981–989.
- [9] Yiting Cheng, Fangyun Wei, Jianmin Bao, Dong Chen, and Wenqiang Zhang. 2023. Cico: Domain-aware sign language retrieval via cross-lingual contrastive learning. In *Proceedings of the IEEE/CVF Conference on Computer Vision and Pattern Recognition*. 19016–19026.
- [10] Joon Son Chung and Andrew Zisserman. 2017. Out of time: automated lip sync in the wild. In *Computer Vision—ACCV 2016 Workshops: ACCV 2016 International Workshops, Taipei, Taiwan, November 20–24, 2016, Revised Selected Papers, Part II 13*. Springer, 251–263.
- [11] Martin Cooke, Jon Barker, Stuart Cunningham, and Xu Shao. 2006. An audio-visual corpus for speech perception and automatic speech recognition. *The Journal of the Acoustical Society of America* 120, 5 (2006), 2421–2424.
- [12] Wanxia Deng, Lingjun Zhao, Qing Liao, Deke Guo, Gangyao Kuang, Dewen Hu, Matti Pietikäinen, and Li Liu. 2021. Informative feature disentanglement for unsupervised domain adaptation. *IEEE Transactions on Multimedia* 24 (2021), 2407–2421.
- [13] Han Fang, Pengfei Xiong, Luhui Xu, and Yu Chen. 2021. Clip2video: Mastering video-text retrieval via image clip. *arXiv preprint arXiv:2106.11097* (2021).
- [14] Yaroslav Ganin, Evgeniya Ustinova, Hana Ajakan, Pascal Germain, Hugo Larochelle, François Laviolette, Mario March, and Victor Lempitsky. 2016. Domain-adversarial training of neural networks. *Journal of machine learning research* 17, 59 (2016), 1–35.
- [15] Yi He, Lei Yang, Hanyi Wang, Yun Zhu, and Shilin Wang. 2024. Speaker-Adaptive Lipreading Via Spatio-Temporal Information Learning. In *ICASSP 2024 - 2024 IEEE International Conference on Acoustics, Speech and Signal Processing (ICASSP)*. 10411–10415.
- [16] Yiyang Huang, Xuefeng Liang, and Chaowei Fang. 2021. Callip: Lipreading using contrastive and attribute learning. In *Proceedings of the 29th ACM International Conference on Multimedia*. 2492–2500.
- [17] Minsu Kim, Hyunjun Kim, and Yong Man Ro. 2022. Speaker-Adaptive Lip Reading with User-Dependent Padding. In *Computer Vision – ECCV 2022*. Springer Nature Switzerland, Cham, 576–593.
- [18] Minsu Kim, Jeong Hun Yeo, Jeongsoo Choi, and Yong Man Ro. 2023. Lip reading for low-resource languages by learning and combining general speech knowledge and language-specific knowledge. In *Proceedings of the IEEE/CVF International Conference on Computer Vision*. 15359–15371.
- [19] Yaman Kumar, Rohit Jain, Khwaja Mohd Salik, Rajiv Ratn Shah, Yifang Yin, and Roger Zimmermann. 2019. Lipper: Synthesizing thy speech using multi-view lipreading. In *Proceedings of the AAAI Conference on artificial intelligence*, Vol. 33. 2588–2595.
- [20] Junnan Li, Dongxu Li, Silvio Savarese, and Steven Hoi. 2023. Blip-2: Bootstrapping language-image pre-training with frozen image encoders and large language

- models. In *International conference on machine learning*. PMLR, 19730–19742.
- [21] Zhengyang Li, Timo Lohrenz, Matthias Dunkelberg, and Tim Fingscheidt. 2023. Transformer-Based Lip-Reading with Regularized Dropout and Relaxed Attention. In *2022 IEEE Spoken Language Technology Workshop (SLT)*. 723–730.
 - [22] Dongnan Liu, Chaoyi Zhang, Yang Song, Heng Huang, Chenyu Wang, Michael Barnett, and Weidong Cai. 2022. Decompose to adapt: Cross-domain object detection via feature disentanglement. *IEEE Transactions on Multimedia* 25 (2022), 1333–1344.
 - [23] Huaishao Luo, Lei Ji, Ming Zhong, Yang Chen, Wen Lei, Nan Duan, and Tianrui Li. 2022. Clip4clip: An empirical study of clip for end to end video clip retrieval and captioning. *Neurocomputing* 508 (2022), 293–304.
 - [24] Songtao Luo, Shuang Yang, Shiguang Shan, and Xilin Chen. 2023. Learning Separable Hidden Unit Contributions for Speaker-Adaptive Lip-Reading. (2023).
 - [25] Pingchuan Ma, Brais Martinez, Stavros Petridis, and Maja Pantic. 2021. Towards practical lipreading with distilled and efficient models. In *ICASSP 2021-2021 IEEE International Conference on Acoustics, Speech and Signal Processing (ICASSP)*. IEEE, 7608–7612.
 - [26] Xinghua Ma and Shilin Wang. 2022. Chinese Mandarin Lipreading using Cascaded Transformers with Multiple Intermediate Representations. In *2022 IEEE International Conference on Image Processing (ICIP)*. 2561–2565.
 - [27] Brais Martinez, Pingchuan Ma, Stavros Petridis, and Maja Pantic. 2020. Lipreading using temporal convolutional networks. In *ICASSP 2020-2020 IEEE International Conference on Acoustics, Speech and Signal Processing (ICASSP)*. IEEE, 6319–6323.
 - [28] Ziling Miao, Hong Liu, and Bing Yang. 2020. Part-based lipreading for audio-visual speech recognition. In *2020 IEEE International Conference on Systems, Man, and Cybernetics (SMC)*. IEEE, 2722–2726.
 - [29] Xuesong Niu, Zitong Yu, Hu Han, Xiaobai Li, Shiguang Shan, and Guoying Zhao. 2020. Video-based remote physiological measurement via cross-verified feature disentanglement. In *Computer Vision—ECCV 2020: 16th European Conference, Glasgow, UK, August 23–28, 2020, Proceedings, Part II 16*. Springer, 295–310.
 - [30] Stavros Petridis, Themis Stafylakis, Pingchuan Ma, Feipeng Cai, Georgios Tzimiropoulos, and Maja Pantic. 2018. End-to-end audiovisual speech recognition. In *2018 IEEE international conference on acoustics, speech and signal processing (ICASSP)*. IEEE, 6548–6552.
 - [31] Javad Peymanfard, Mohammad Reza Mohammadi, Hossein Zeinali, and Nasser Mozayani. 2022. Lip reading using external viseme decoding. In *2022 International Conference on Machine Vision and Image Processing (MVIP)*. IEEE, 1–5.
 - [32] KR Prajwal, Triantafyllos Afouras, and Andrew Zisserman. 2022. Sub-word level lip reading with visual attention. In *Proceedings of the IEEE/CVF Conference on Computer Vision and Pattern Recognition*. 5162–5172.
 - [33] Alec Radford, Jong Wook Kim, Chris Hallacy, Aditya Ramesh, Gabriel Goh, Sandhini Agarwal, Girish Sastry, Amanda Askell, Pamela Mishkin, Jack Clark, et al. 2021. Learning transferable visual models from natural language supervision. In *International conference on machine learning*. PMLR, 8748–8763.
 - [34] Alec Radford, Jong Wook Kim, Tao Xu, Greg Brockman, Christine McLeavey, and Ilya Sutskever. 2023. Robust speech recognition via large-scale weak supervision. In *International conference on machine learning*. PMLR, 28492–28518.
 - [35] Sucheng Ren, Yong Du, Jianming Lv, Guoqiang Han, and Shengfeng He. 2021. Learning from the master: Distilling cross-modal advanced knowledge for lip reading. In *Proceedings of the IEEE/CVF Conference on Computer Vision and Pattern Recognition*. 13325–13333.
 - [36] Joon Son Chung, Andrew Senior, Oriol Vinyals, and Andrew Zisserman. 2017. Lip reading sentences in the wild. In *Proceedings of the IEEE conference on computer vision and pattern recognition*. 6447–6456.
 - [37] Ilya Sutskever, Oriol Vinyals, and Quoc V Le. 2014. Sequence to sequence learning with neural networks. *Advances in neural information processing systems* 27 (2014).
 - [38] Jianyi Wang, Kelvin CK Chan, and Chen Change Loy. 2023. Exploring clip for assessing the look and feel of images. In *Proceedings of the AAAI Conference on Artificial Intelligence*, Vol. 37. 2555–2563.
 - [39] Tao Wang, Hong Liu, Pinhao Song, Tianyu Guo, and Wei Shi. 2022. Pose-guided feature disentanglement for occluded person re-identification based on transformer. In *Proceedings of the AAAI conference on artificial intelligence*, Vol. 36. 2540–2549.
 - [40] Bo Xu, Cheng Lu, Yandong Guo, and Jacob Wang. 2020. Discriminative multi-modality speech recognition. In *Proceedings of the IEEE/CVF Conference on Computer Vision and Pattern Recognition*. 14433–14442.
 - [41] Jingyi Xu, Hieu Le, Mingzhen Huang, ShahRukh Athar, and Dimitris Samaras. 2021. Variational feature disentanglement for fine-grained few-shot classification. In *Proceedings of the IEEE/CVF international conference on computer vision*. 8812–8821.
 - [42] Kai Xu, Dawei Li, Nick Cassimatis, and Xiaolong Wang. 2018. LCArNet: End-to-end lipreading with cascaded attention-CTC. In *2018 13th IEEE International Conference on Automatic Face & Gesture Recognition (FG 2018)*. IEEE, 548–555.
 - [43] Feng Xue, Yu Li, Deyin Liu, Yincen Xie, Lin Wu, and Richang Hong. 2023. Lip-former: learning to lipread unseen speakers based on visual-landmark transformers. *IEEE Transactions on Circuits and Systems for Video Technology* 33, 9 (2023), 4507–4517.
 - [44] Feng Xue, Tian Yang, Kang Liu, Zikun Hong, Mingwei Cao, Dan Guo, and Richang Hong. 2023. Lcsnet: End-to-end lipreading with channel-aware feature selection. *ACM Transactions on Multimedia Computing, Communications and Applications* 19, 1s (2023), 1–21.
 - [45] Xiaobing Zhang, Haigang Gong, Xili Dai, Fan Yang, Nianbo Liu, and Ming Liu. 2019. Understanding Pictograph with Facial Features: End-to-End Sentence-Level Lip Reading of Chinese. *Proceedings of the AAAI Conference on Artificial Intelligence* 33, 01 (Jul. 2019), 9211–9218. doi:10.1609/aaai.v33i01.33019211
 - [46] Yuanhang Zhang, Shuang Yang, Shiguang Shan, and Xilin Chen. 2024. ES3: Evolving Self-Supervised Learning of Robust Audio-Visual Speech Representations. In *Proceedings of the IEEE/CVF Conference on Computer Vision and Pattern Recognition*. 27069–27079.
 - [47] Ya Zhao, Rui Xu, and Mingli Song. 2019. A cascade sequence-to-sequence model for chinese mandarin lip reading. In *Proceedings of the ACM Multimedia Asia*. 1–6.
 - [48] Y. Zhao, R. Xu, X. Wang, P. Hou, H. Tang, and M. Song. 2019. Hearing Lips: Improving Lip Reading by Distilling Speech Recognizers.
 - [49] Benjia Zhou, Zhigang Chen, Albert Clapés, Jun Wan, Yanyan Liang, Sergio Escalera, Zhen Lei, and Du Zhang. 2023. Gloss-free sign language translation: Improving from visual-language pretraining. In *Proceedings of the IEEE/CVF International Conference on Computer Vision*. 20871–20881.